

Article

Electrical Manipulation of Electromagnetically Induced Transparency for Slow Light Purpose Based on Metal-Graphene Hybrid Metamaterial

Chenxi Liu ¹, Song Zha ^{1,*}, Peiguo Liu ¹, Cheng Yang ² and Qihui Zhou ¹ 

¹ College of Electronic Science, National University of Defense Technology, Changsha 410073, China; liuchenxi09@nudt.edu.cn (C.L.); pg731@126.com (P.L.); zhouqihui10@126.com (Q.Z.)

² State Key Laboratory of Millimeter Waves, School of Information Science and Engineering, Southeast University, Nanjing 211189, China; cheng_yang@seu.edu.cn

* Correspondence: zhasong@nudt.edu.cn

Received: 3 November 2018; Accepted: 14 December 2018; Published: 18 December 2018



Featured Application: Slow light devices.

Abstract: A terahertz metamaterial is presented and numerically investigated to achieve tunable electromagnetically induced transparency (EIT) for slow light. The unit cell consists of cut-wire pairs and U-shaped ring resonators with graphene strips placed between the metal film and the SiO₂/Si substrate. Through bright-dark mode coupling, the radiative resonance induced by the U-shaped ring is suppressed, and then the typical EIT effect is realized. The transparency window and the accompanied group delay can be electrically manipulated with different Fermi energy of the graphene. By analyzing the surface distribution, the underlying tuning mechanism of this hybrid metamaterial is investigated in detail. Moreover, the transparency peak decreases slightly with the increasing strip width of the graphene layer but completely vanishes as the strip width exceeds the length of the covered U-shaped ring. The influence of the critical index of graphene quality, i.e., carrier mobility on the EIT effect, is considered. The results of this study may provide valuable guidance in designing and analyzing tunable EIT structures based on a metal-graphene hybrid structure for slow light purposes.

Keywords: metamaterial; electromagnetically induced transparency; graphene; slow light

1. Introduction

The past decade has witnessed great developments in the artificially engineered material metamaterial, which has attracted extensive interests due to its unique electromagnetic properties [1]. Tailored in diverse architectures, metamaterials provide opportunities to control the electromagnetic wave in a wide range, from microwave to near-infrared regions [2–4]. Potential applications are reported in different fields including absorbers, filters, antennas, and polarizers. Recently, researchers have demonstrated that the metamaterial can mimic the electromagnetically induced transparency (EIT) in an atomic system, which refers to a quantum interference that renders a narrow transparent window within an opaque medium [5–7]. The metamaterial analogue of the EIT effect effectively frees researchers from the cumbersome experimental conditions in an atom system, such as low temperatures and pumping lasers. Moreover, it overcomes the restriction of operation frequency range. The EIT effect in metamaterials mainly results from two interference pathways: bright-dark mode coupling and bright-bright mode coupling [8]. Since the earlier study was fulfilled by Zhang et al., various metamaterial designs are proposed and demonstrated to achieve the EIT effect with broadband,

multiple transparency windows and polarization-insensitive properties [9–13]. The imitation of EIT is useful in applications such as slow light, modulating, and sensing purposes [14].

In practical occasions, it is desirable to actively control the EIT effect after the structures are fabricated. Various techniques such as thermal tuning, optical control, and micro-electromechanical (MEMS) systems have been employed to achieve the dynamic manipulation of the EIT metamaterials [15–17]. Among all approaches, electrical modulation is one of the most convenient methods in actual operations. Graphene, a two-dimensional material with carbon atoms arranged in a hexagonal lattice, promises a good candidate as its surface conductivity can be tuned by changing the Fermi energy via external voltages [18,19]. Graphene can interact strongly with both the electromagnetic waves and the adjacent metal patterns when integrated in the metamaterial. In the past few years, a series of graphene-based metamaterial designs have been investigated to achieve the dynamic control of the EIT effect, exhibiting potential applications in controllable buffers and optical modulators [20–24]. Nevertheless, despite extensive studies on the dynamic response of the graphene-based structure, the deformation of the EIT window in the modulating process has not been fully investigated. On the other hand, a large adjustment in Fermi energy is required when tuning the group delay spectra. This may lead to practical difficulty since higher external energy is required. Thus, it is essential to get insight into the tuning mechanisms and improve the design of the dynamically tunable graphene-based EIT structure.

In this work, we present a metal-graphene hybrid metamaterial composed of metal cut-wires and U-shaped rings as well as graphene strips. Numerical investigations of the transmission spectra are systematically conducted. The transparency peak is induced via the interactions between the U-shaped ring and the cut-wire pairs under terahertz illumination. As a graphene layer is inserted under the metal patterns, the transmission of the metamaterial decreases drastically and the EIT effect is seriously weakened. When increasing the Fermi energy, the transparency window manifests an evident deformation with distinctive variations in the transmission peak and dips. The surface current distribution on the metamaterial is analyzed to investigate the tuning mechanism of the deformed window. Furthermore, the slow light effect accompanied with the EIT phenomenon can also be modulated with different Fermi energy. Compared with previous works, the tunable slow light performance requires small values and slight changes in the Fermi energy of graphene, which provide more feasibility in practical operation.

2. Geometric Structure and Graphene Model

The schematic and unit cell of the metal-graphene hybrid structure are depicted in Figure 1. The metal resonator arranged in periodic array contains a pair of gold cut-wires and a U-shaped ring located between the cut-wires. The geometrical parameters of the EIT metamaterial have been optimized and defined as shown in Figure 1b. The periodic length of the unit cell is $P_x = P_y = 100 \mu\text{m}$. The displacement between the unit center and the U-shaped ring is defined as $s = 2 \mu\text{m}$. The graphene strip with a width of $w_1 = 22 \mu\text{m}$ is placed between the metal patterns and the SiO_2/Si substrate. The thickness of the silicon dioxide is 100 nm and the thickness of the silicon layer is 1 μm . Other structural parameters are as follows: $l_1 = 50 \mu\text{m}$, $l_2 = 36 \mu\text{m}$, $l_3 = 15 \mu\text{m}$, $w_2 = 6 \mu\text{m}$, $w_3 = 3 \mu\text{m}$, and $g = 15 \mu\text{m}$. The graphene strips are connected to the gold film as the top electrode and the other electrode is on the side of the silicon substrate. Therefore, the bias voltages can be applied between the electrodes to tune the Fermi energy in graphene as shown in Figure 1a.

The graphene is modeled as an infinitesimally thin film and its surface conductivity in the lower-THz region is dominated by the intraband transitions, which can be expressed using the well-known Kubo formula [25]:

$$\sigma_{\text{intra}}(\omega, E_F, \tau, T) = j \frac{e^2 k_B T}{\pi \hbar^2 (\omega + j\tau^{-1})} \left(\frac{E_F}{k_B T} + 2 \ln \left(e^{\frac{-E_F}{k_B T}} + 1 \right) \right) \quad (1)$$

where k_B and \hbar are the Boltzmann constant and the reduced Planck constant, respectively, T is the temperature, E_F is the Fermi energy in graphene, ω is the operation circular frequency, and e is the electron charge. τ is the carrier scattering time in graphene, which is related to carrier mobility μ , and Fermi energy according to $\mu = E_F v_F^2 \tau / e$, $v_F = 10^6$ m/s is the Fermi velocity. Here, we assumed $\mu = 3000$ cm² V⁻¹ s⁻¹, which is a compromise value lower than the experimental results in refs. [26,27].

By applying an external voltage V_g , the Fermi energy of the graphene layer can be actively tuned. For our structure, an approximate relation between E_F and V_g can be derived using a simple theoretical capacitor model which is presented by [28,29]:

$$E_F = \hbar v_F \sqrt{\pi \epsilon_0 \epsilon_r |V_g - V_d| / e d_s} \quad (2)$$

where ϵ_0 is the permittivity of the vacuum, ϵ_r is the permittivity of the silicon dioxide, V_d is the Dirac point voltage, and d_s is the thickness of the silicon dioxide layer.

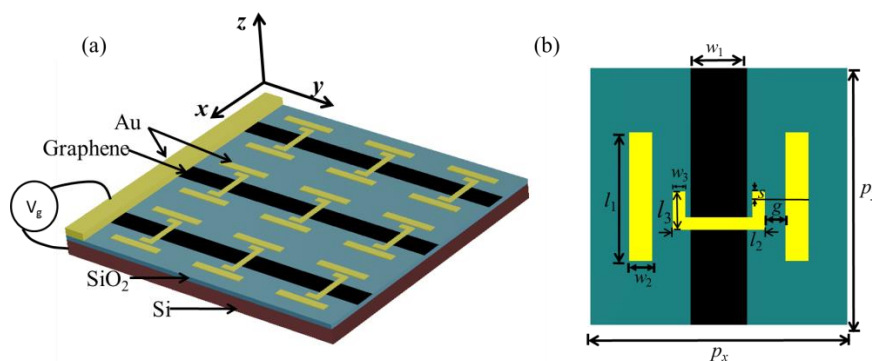


Figure 1. (a) The geometrical schematic of the proposed metal-graphene metamaterial and (b) the unit cell of the structure.

3. Results and Discussions

In order to explore the response of the hybrid metamaterial, the numerical calculations are performed based on the frequency domain method and employing the electromagnetic simulation software CST Microwave Studio based on the frequency domain Finite Element Method. The terahertz wave normally illuminates on the structure along z direction with linear polarization in x direction. The unit cell boundary conditions are utilized in both x and y directions and the open boundary conditions are utilized in z direction. The investigated frequency range is from 1.0 to 2.4 THz.

Figure 2 shows the transmission spectra of the sole U-shaped ring, the sole cut-wire pair, the combined structure, and the hybrid structure with the graphene layer. It can be seen that the U-shaped ring manifests a single resonance with a transmission dip at 1.74 THz, which can serve as bright mode. By contrast, the cut-wire pairs display a near-unity transmission under the terahertz illumination in the investigated range, which can be considered as dark mode. When the two resonators are combined in the same unit cell, a noticeable transparency window appears while the transmission dip splits to two branches, indicating an evident EIT behavior. Moreover, for the hybrid structure with a graphene layer positioned between the substrate and the U-shaped resonator, the EIT effect is drastically damped and the transmission amplitude experiences an evident decline. The Fermi energy of graphene is 0.05 eV.

To understand the physical mechanism of the EIT effect, the electric field distributions of the isolated resonators and the combined structure with/without graphene layer are calculated. Figure 3 shows the electric field distribution at the transmission dips and the transparency peaks, which are labeled in Figure 2. It is observed that the U-shaped ring can be directly excited by the incident wave. The field distribution of the isolated cut-wire pair is not shown as the field amplitude is much smaller compared with those of other circumstances, implying inactive behaviour under illumination. At transmission dips of the combined structure, the cut-wire pair is excited indirectly with the near-field interaction between two resonators, as shown in Figure 3b,c. At the transmission peak, the electric field

locates mainly on the edge of the cut-wire pairs and the initial radiative element, i.e., the U-shaped rings, are not induced, as can be seen in Figure 3d. This indicates a destructive interference between two resonators and thus the radiative mode is suppressed. Moreover, with the graphene layer placed under the U-shaped ring, there exists more electric field concentrated on the edges of the graphene strip and the U-shaped ring, which results in the noticeable attenuation at the transparency peak.

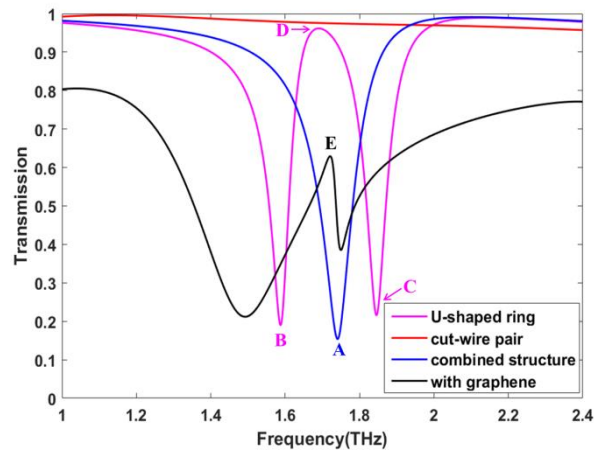


Figure 2. Transmission spectra of the sole U-shaped ring, the sole cut-wire pair, the combined structure, and the hybrid structure with a graphene layer.

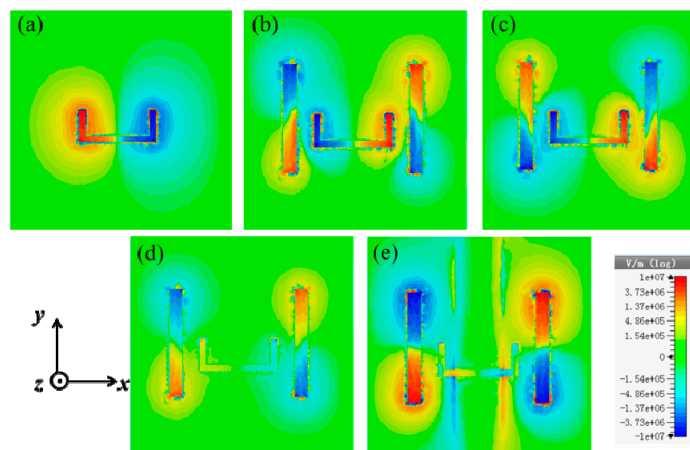


Figure 3. (a–e) The electric field distribution at the resonant frequency corresponding to Figure 2 labelled A, B, C, D, E, respectively. The Fermi energy of the graphene layer is 0.05 eV.

As mentioned above, by applying external voltages, the Fermi energy and the surface conductivity of the graphene layer can be dynamically tuned, thus the modulation of the spectral EIT window can be realized. The transmission spectra with different Fermi energy in graphene are calculated and plotted in Figure 4. It can be seen that as the Fermi energy increases, the EIT window is gradually damped and the resonance frequencies manifest red shift. The first transmission dip increases drastically from 0.21 to 0.50 as the Fermi energy is tuned from 0.05 eV to 0.15 eV, meanwhile the other dip and the transmission peak experience slight fluctuations. When increasing the Fermi energy to a maximum value of 0.20 eV, the transmission dips gradually disappear and consequently the EIT window vanishes. The distinctive variations that occur in the transmission peak and dips lead to the deformed transparency window of the hybrid metamaterial. It is worth noting that in our hybrid metamaterial, the graphene layer is placed right between the U-shaped ring and the substrate, and this design causes strong coupling between the graphene strip and the radiative resonator, which accounts for the complete deformation of the EIT window.

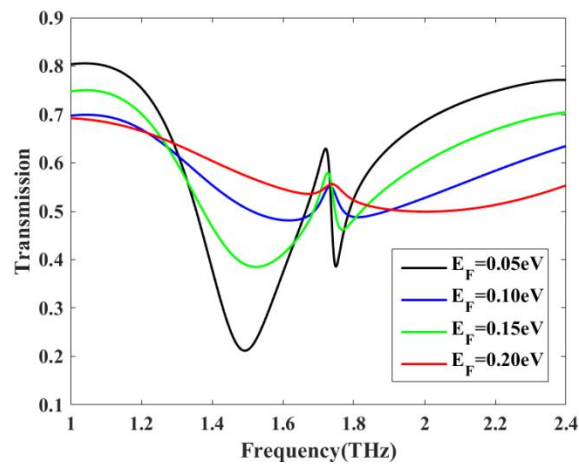


Figure 4. Transmission spectra of the hybrid metamaterial with different Fermi energy.

To interpret the distinctive amplitude variations in different resonances, the surface current distribution at the transparency peak (1.71 THz) and the transmission dips (1.49 THz and 1.75 THz) with $E_F = 0.05$ eV and $E_F = 0.20$ eV are calculated and plotted in Figure 5. It is obvious from Figure 5a,d that the surface current intensity on the U-shaped resonator is weakened as E_F rises from 0.05 to 0.20 eV. As $E_F = 0.20$ eV, more electron-hole pair recombination occurs in the graphene layer, which renders the surface currents no longer concentrated on the U-shaped ring. As a consequence, the radiative mode is suppressed and the amplitude of the first transmission dip drastically increases. A similar phenomenon is observed at the second transmission dip, as shown in Figure 5c,f, despite the relatively slight changes in the surface current intensity. The attenuation of the current intensity is also observed, as shown in Figure 5b,e. Nevertheless, the intensity variation is rather small at the transmission peak and the amplitude exhibits a slight decrease because of the enhanced radiative loss caused by the more conductive graphene strip with higher Fermi energy.

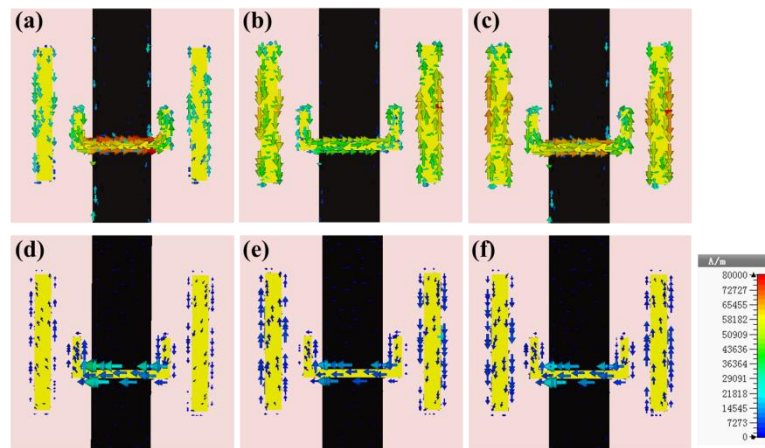


Figure 5. The calculated surface current distributions of the proposed metamaterial at transmission peak and dips with different Fermi energy. (a–c) $f = 1.49, 1.71, 1.75$ THz as $E_F = 0.05$ eV; (d–f) $f = 1.49, 1.71, 1.75$ THz as $E_F = 0.20$ eV.

The EIT effect with dispersive curves can lead to the slow light behavior. The slow light capability can be characterized by the group delay of the transmitted wave, which can be defined as $t_g = -d\varphi/d\omega$, where φ is the transmission phase and ω is the operation frequency. Figure 6a depicts the group delay spectra of the metamaterial with and without the graphene layer. The positive and negative values denote the slow and fast light effects, respectively. Apparently, without the graphene strip, a broadband slow-light region and a group delay up to 2.2 ps are realized. As the graphene layer is

placed between the U-shaped ring and the substrate, the slow light region is drastically narrowed but the maximum value of group delay is increased to 3.3 ps. Moreover, by applying gate voltages, the dynamical control of the group delay can be achieved based on the hybrid structure. With the Fermi energy increasing from 0.05 to 0.20 eV, the group delay is reduced from 3.3 to 0.5 ps and the metamaterial gradually loses the slow light capability. It is noted that the adjustment to the Fermi energy required for group delay modulation is much smaller than that in ref. [21–24], which may provide more feasibility in practical operation. This feature is due to the strong coupling caused by the direct contact between the graphene layer and the U-shaped ring in our design. The external voltages required for tuning the Fermi energy based on our structure can approximately be evaluated according to Equation (2). Assuming the Dirac point voltage $V_d = 0$ V, the relation between the gate voltages and the tuning range of Fermi energy is calculated and plotted. From Figure 6b, we can evaluate that when external voltages are changed from 0.9 to 14 V, the Fermi energy is tuned from 0.05 to 0.20 eV, thus the group delay of the metamaterial can be reduced from 3.3 to 0.5 ps. Therefore, the active modulation of the slow light effect can be realized, which is highly desirable in terahertz communication.

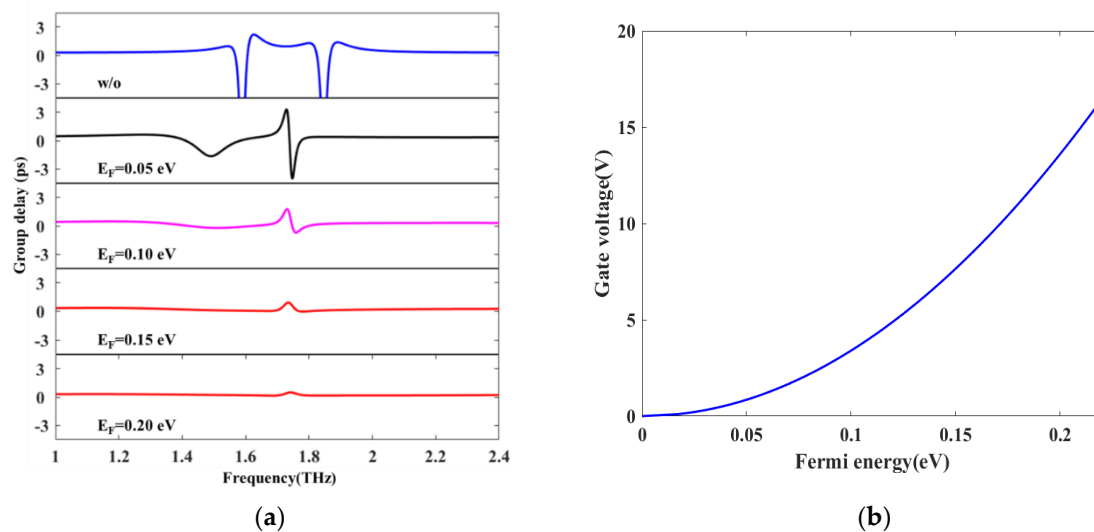


Figure 6. (a) The group delay of the hybrid metamaterial with and without the graphene layer; (b) the approximate relation between the gate voltages and the Fermi energy.

To further investigate the influence of the graphene layer, the responses of the metamaterial with the width of the graphene strip increasing from 22 to 42 μm are calculated and depicted in Figure 7. The Fermi energy is fixed at 0.05 eV. The transmission amplitude of the whole transparency window declines gradually when the size of the graphene layer is increased. Intriguingly, there exists a remarkable difference between the two circumstances when the strip width is more and less than the U-shaped ring length l_2 . The transparency window remains noticeable regardless of degradation as the strip width is less than l_2 . However, if the width is larger than l_2 , the amplitude of the transparency dips sharply rises and the EIT effect almost disappears. As the U-shaped ring and the substrate are completely separated by the graphene layer, the complete interaction between the bright resonator and the graphene strip destroys the radiative mode. This destruction accounts for the sharp increase of transmission dips and the vanishing of the EIT window.

As can be inferred from the transmission spectra in Figure 7, the strip width of the graphene layer can also have a significant impact on the slow light effect. Figure 8 shows the variations of the group delay spectra with different strip widths. It is interesting to see that the group delay manifests a slight increase from 3.6 to 3.7 ps as the strip width rises from 27 to 32 μm . The enhanced interaction between the graphene layer and the U-shaped ring arising from the wider strip may account for the larger group delay. As the strip width becomes larger than U-shaped ring length, the group delay sharply declines to a much smaller value of 1.4 ps, which coincides with the vanishing trend of the

transparency window depicted in Figure 7. The slow light effect disappears when the strip width further increases to 42 μm . Therefore, the optical buffering performance of the hybrid structure can be completely switched through changing the width of the graphene strip.

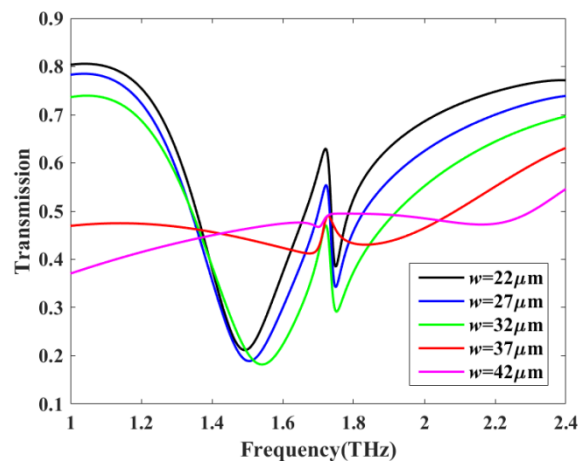


Figure 7. Transmission spectra of metamaterial with different widths of the graphene strip.

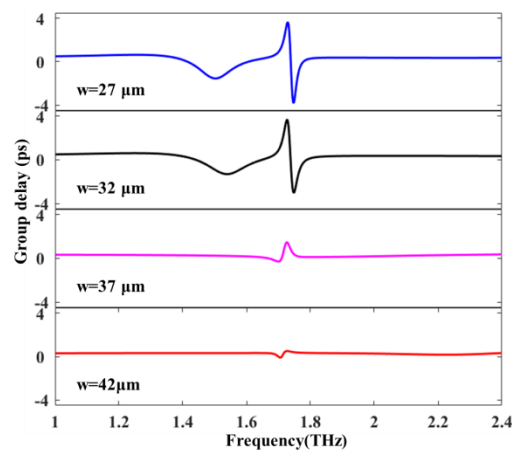


Figure 8. The group delay of the hybrid metamaterial with different widths of the graphene strip.

As is well known, the carrier mobility is a critical index of graphene quality, which is closely related to the surface conductivity. In practice, it is a variable dependent on the production process. Here, the effect of the carrier mobility on the spectral response of the EIT metamaterial is investigated, which has seldom been reported as far as we know. The Fermi energy of the graphene strip is fixed at 0.10 eV. Figure 9a shows the transmission spectra of the proposed structure with carrier mobility μ in the graphene varying from 2000 to 4000 $\text{cm}^2 \text{V}^{-1} \text{s}^{-1}$. It can be seen that as μ increases, the transparency peak declines slightly while the amplitude of transmission dips gradually rises, indicating the weakening of the EIT phenomenon. This trend is similar with the circumstance when the Fermi energy is increased, since the surface conductivity is enhanced with higher carrier mobility. Moreover, the group delay spectra with different carrier mobility are calculated, as depicted in Figure 9b. A noticeable decrease in the group delay can be observed, and the maximum value is reduced from 2.1 to 1.4 ps as μ increases from 2000 to 4000 $\text{cm}^2 \text{V}^{-1} \text{s}^{-1}$. It is worth noting that larger variations of the carrier mobility can lead to more drastic fluctuations in both the transmission and the group delay spectra. Therefore, the carrier mobility is an essential factor for the metal-graphene hybrid metamaterial in realizing the EIT window and the corresponding slow light performance.

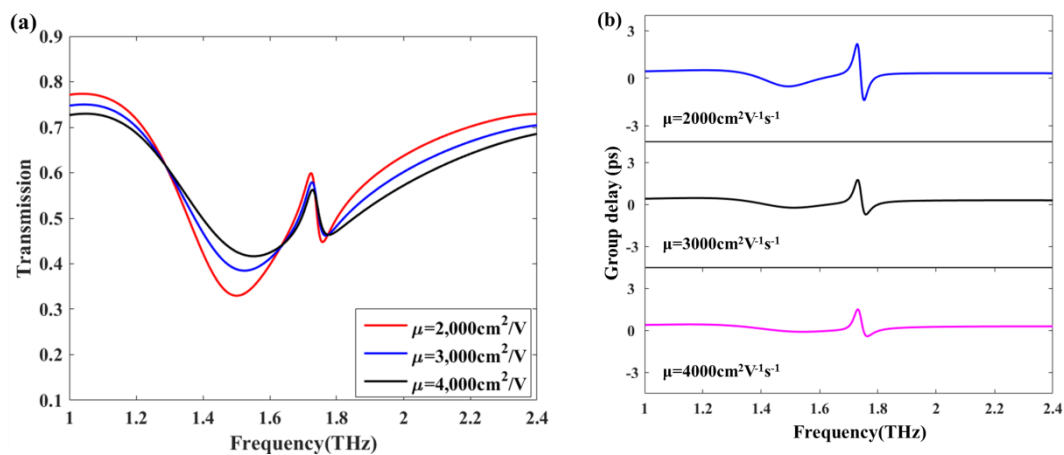


Figure 9. (a) The transmission and (b) group delay spectra of the hybrid metamaterial with different carrier mobility in graphene.

4. Conclusions

In summary, the dynamic manipulation of the metal-graphene hybrid structure has been theoretically proposed and numerically investigated. The transparency window is substantially weakened with the presence of the graphene layer and can be actively modulated by tuning the Fermi energy via external voltages. The distinctive variations in different resonances of the transparency window as Fermi energy changes are elucidated by analyzing the surface current distribution. The different width of the strip is considered to explore the influence of the graphene layer. Moreover, the tunable slow light effect is analyzed in detail with various parameters including Fermi energy, strip width, and carrier mobility. The proposed metamaterial may be useful in designing terahertz modulators and optical buffers, and the presented analysis of the physical manipulation mechanism can be significant in developing devices based on the metal-graphene hybrid structure in the THz regime, which can also be extended to other spectral regimes.

Author Contributions: Conceptualization, C.L.; Data curation, S.Z.; Formal analysis, S.Z. and C.Y.; Investigation, C.L.; Methodology, C.L.; Project administration, S.Z.; Resources, C.Y.; Software, C.L.; Supervision, P.L.; Visualization, Q.Z.; Writing—original draft, C.L.; Writing—review & editing, C.L., S.Z. and P.L.

Funding: This research received no external funding.

Conflicts of Interest: The authors declare no conflict of interest.

References

- Smith, D.R.; Pendry, J.B.; Wiltshire, M.C. Metamaterials and negative refractive index. *Science* **2004**, *305*, 788–792. [[CrossRef](#)] [[PubMed](#)]
- Yoo, M.; Lim, S. Polarization-independent and ultrawideband metamaterial absorber using a hexagonal artificial impedance surface and a resistor-capacitor layer. *IEEE Trans. Antennas Propag.* **2014**, *62*, 2652–2658.
- Staude, I.; Schilling, J. Metamaterial-inspired silicon nanophotonics. *Nat. Photon.* **2017**, *11*, 274–284. [[CrossRef](#)]
- Yao, G.; Ling, F.; Yue, J.; Luo, C.; Ji, J.; Yao, J. Dual-band tunable perfect metamaterial absorber in the THz range. *Opt. Express* **2016**, *24*, 1518–1527. [[CrossRef](#)] [[PubMed](#)]
- Harris, S.E. Dispersive properties of electromagnetically induced transparency. *Phys. Rev. A* **1992**, *49*, 29–32. [[CrossRef](#)]
- Marcinkevičius, S.; Gushterov, A.; Reithmaier, J.P. Transient electromagnetically induced transparency in self-assembled quantum dots. *Appl. Phys. Lett.* **2008**, *92*, 041113.

7. Liu, N.; Weiss, T.; Mesch, M.; Langguth, L.; Eigenthaler, U.; Hirscher, M.; Sönnichsen, C.; Giessen, H. Planar metamaterial analogue of electromagnetically induced transparency for plasmonic sensing. *Nano Lett.* **2010**, *10*, 1103–1107. [[CrossRef](#)] [[PubMed](#)]
8. Jin, X.R.; Park, J.; Zheng, H.; Lee, S.; Lee, Y.P.; Rhee, J.Y.; Kim, K.W.; Cheong, H.S.; Jang, W.H. Highly-dispersive transparency at optical frequencies in planar metamaterials based on two-bright-mode coupling. *Opt. Express* **2011**, *19*, 21652–21657. [[CrossRef](#)] [[PubMed](#)]
9. Zhang, S.; Genov, D.A.; Wang, Y.; Liu, M.; Zhang, X. Plasmon-induced transparency in metamaterials. *Phys. Rev. Lett.* **2008**, *101*, 047401. [[CrossRef](#)] [[PubMed](#)]
10. Li, H.; Liu, S.B.; Liu, S.Y.; Zhang, H. Electromagnetically induced transparency with large group index induced by simultaneously exciting the electric and the magnetic resonance. *Appl. Phys. Lett.* **2014**, *105*, 133514. [[CrossRef](#)]
11. Liu, M.; Yang, Q.; Xu, Q.; Chen, X.; Tian, Z.; Gu, J.; Ouyang, C.; Zhang, X.; Han, J.; Zhang, W. Tailoring mode interference in plasmon-induced transparency metamaterials. *J. Phys. D Appl. Phys.* **2018**, *51*, 174005. [[CrossRef](#)]
12. Yin, X.G.; Feng, T.; Yip, S.; Liang, X.; Hui, A.; Ho, J.C.; Li, J. Tailoring electromagnetically induced transparency for terahertz metamaterials from diatomic to triatomic structural molecules. *Appl. Phys. Lett.* **2013**, *103*, 021115. [[CrossRef](#)]
13. Wan, M.; Song, Y.; Zhang, L.; Zhou, F. Broadband plasmon-induced transparency in terahertz metamaterials via constructive interference of electric and magnetic couplings. *Opt. Express* **2015**, *23*, 27361. [[CrossRef](#)] [[PubMed](#)]
14. Zhu, L.; Meng, F.; Fu, J.; Wu, Q. An electromagnetically induced transparency metamaterial with polarization insensitivity based on multi-quasi-dark modes. *J. Phys. D Appl. Phys.* **2012**, *45*, 445105. [[CrossRef](#)]
15. Duan, X.; Chen, S.; Cheng, H.; Li, Z.; Tian, J. Dynamically tunable plasmonically induced transparency by planar hybrid metamaterial. *Opt. Lett.* **2013**, *38*, 483–485. [[CrossRef](#)]
16. Gu, J.; Singh, R.; Liu, X.; Zhang, X.; Ma, Y.; Zhang, S.; Maier, S.; Tian, Z.; Azad, A.; Chen, H.; et al. Active control of electromagnetically induced transparency analogue in terahertz metamaterials. *Nat. Commun.* **2012**, *3*, 1151. [[CrossRef](#)]
17. Pitchappa, P.; Manjappa, M.; Ho, C.P.; Singh, R.; Singh, N.; Lee, C. Active control of electromagnetically induced transparency analog in terahertz MEMS metamaterial. *Adv. Opt. Mater.* **2016**, *4*, 541–547. [[CrossRef](#)]
18. Novoselov, K.S.; Geim, A.K.; Morozov, S.V.; Jiang, D.; Zhang, Y.; Dubonos, S.V. Electric field effect in atomically thin carbon films. *Science* **2004**, *306*, 666–669. [[CrossRef](#)]
19. Liu, C.; Liu, P.; Yang, C.; Bian, L. Terahertz metamaterial based on dual-band graphene ring resonator for modulating and sensing applications. *J. Opt.* **2017**, *19*, 115102. [[CrossRef](#)]
20. Xiao, S.; Wang, T.; Liu, T.; Yan, X.; Li, Z.; Xu, C. Active modulation of electromagnetically induced transparency analogue in terahertz hybrid metal-graphene metamaterials. *Carbon* **2018**, *126*, 271–278. [[CrossRef](#)]
21. He, X.; Yang, X.; Lu, G.; Yang, W.; Wu, F.; Yu, Z.; Jiang, J. Implementation of selective controlling electromagnetically induced transparency in terahertz graphene metamaterial. *Carbon* **2017**, *123*, 668–675. [[CrossRef](#)]
22. Zhang, H.; Cao, Y.; Liu, Y.; Li, Y.; Zhang, Y. A novel graphene metamaterial design for tunable terahertz plasmon induced transparency by two bright mode coupling. *Opt. Commun.* **2017**, *391*, 9–15. [[CrossRef](#)]
23. Ding, J.; Arigong, B.; Ren, H. Tuneable complementary metamaterial structures based on graphene for single and multiple transparency windows. *Sci. Rep.* **2014**, *4*, 6128. [[CrossRef](#)] [[PubMed](#)]
24. Liu, C.; Liu, P.; Yang, C.; Lin, Y.; Zha, S. Dynamic electromagnetically induced transparency based on a metal-graphene hybrid metamaterial. *Opt. Mater. Express* **2018**, *8*, 1132. [[CrossRef](#)]
25. Tang, W.; Wang, L.; Chen, X.; Liu, C.; Yu, A.; Lu, W. Dynamic metamaterial based on the graphene split ring high-Q Fano-resonator for sensing applications. *Nanoscale* **2016**, *8*, 15196–15204. [[CrossRef](#)]
26. Chen, B.; Huang, H.; Ma, X.; Huang, L.; Zhang, Z.; Peng, L. How good can CVD-grown monolayer graphene be? *Nanoscale* **2014**, *6*, 15255–15261. [[CrossRef](#)]
27. Huard, B.; Stander, N.; Sulpizio, J.; Goldhaber-Gordon, D. Evidence of the role of contacts on the observed electron-hole asymmetry in graphene. *Phys. Rev. B* **2008**, *78*, 121402. [[CrossRef](#)]

28. Esale-Rodriguez, B.; Yan, R.; Rafique, S.; Zhu, M.; Li, W.; Liang, X.; Gundlach, D.; Protasenko, V.; Kelly, M.M.; Jena, D.; et al. Extraordinary control of terahertz beam reflectance in graphene electro-absorption modulators. *Nano Lett.* **2012**, *12*, 4518–4522. [[CrossRef](#)]
29. Ren, L.; Zhang, Q.; Yao, J.; Sun, Z.; Kaneko, R.; Yan, Z.; Nanot, S.; Jin, Z.; Kawayama, I.; Tonouchi, M.; et al. Terahertz and infrared spectroscopy of gated large-area graphene. *Nano Lett.* **2012**, *12*, 3711. [[CrossRef](#)]



© 2018 by the authors. Licensee MDPI, Basel, Switzerland. This article is an open access article distributed under the terms and conditions of the Creative Commons Attribution (CC BY) license (<http://creativecommons.org/licenses/by/4.0/>).